BACKSCATTERING SIGNATURES AT KU BAND OVER AFRICA FROM JASON-3 AND SWIM

Frappart F., Blarel F. , Aoulad Z., Prigent C., Mougin E., Papa F., Paillou P. , Zribi M. , Normandin C. , Zeiger P., Darrozes J., Bourrel L., Moisy C., Wigneron J-P.

Different types of radar sensors

3 different sensor types:

- Scatterometers : global coverage, low spatial resolution, high temporal resolution, medium incidence, σ^0

- SAR : global coverage, high spatial resolution, low temporal resolution (before the launch of Sentinel-1), medium incidence, σ^0

- Altimeters: global coverage but discontinuous (along the tracks), high spatial resolution along-track, low temporal resolution, nadir incidence, R and σ^0

Major environmental applications of radar over land

- Soil roughness: Scatterometers, SAR, altimeters
  Aerodynamic Roughness Length: $z_0 = \exp(A^*\sigma^0 + B)$

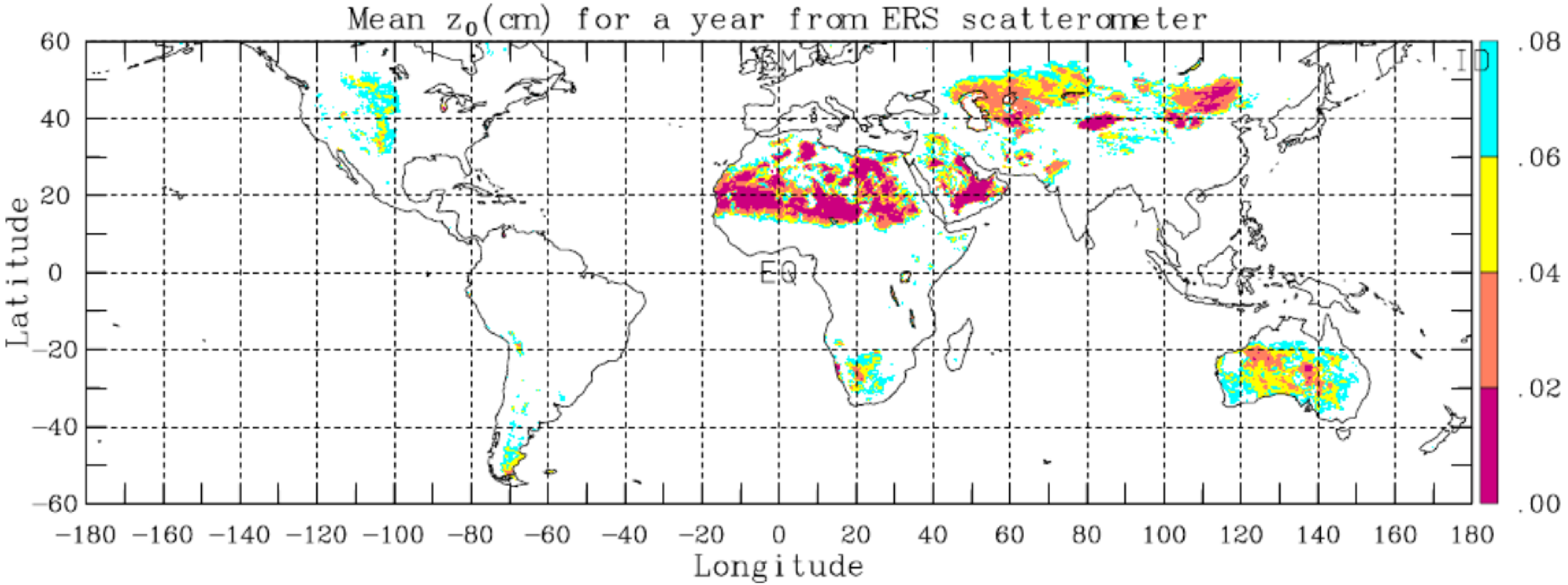

Map of mean z_0 estimated from scatterometer (C-band)

Prigent et al., JGR (2005)

Major environmental applications of radar over land

- Soil moisture estimates : σ^0_{soil}= C * SSM + D from WCM (Attema & Ulaby, 1978)

  Scatterometers, SAR, altimeters (over semi-arid areas)

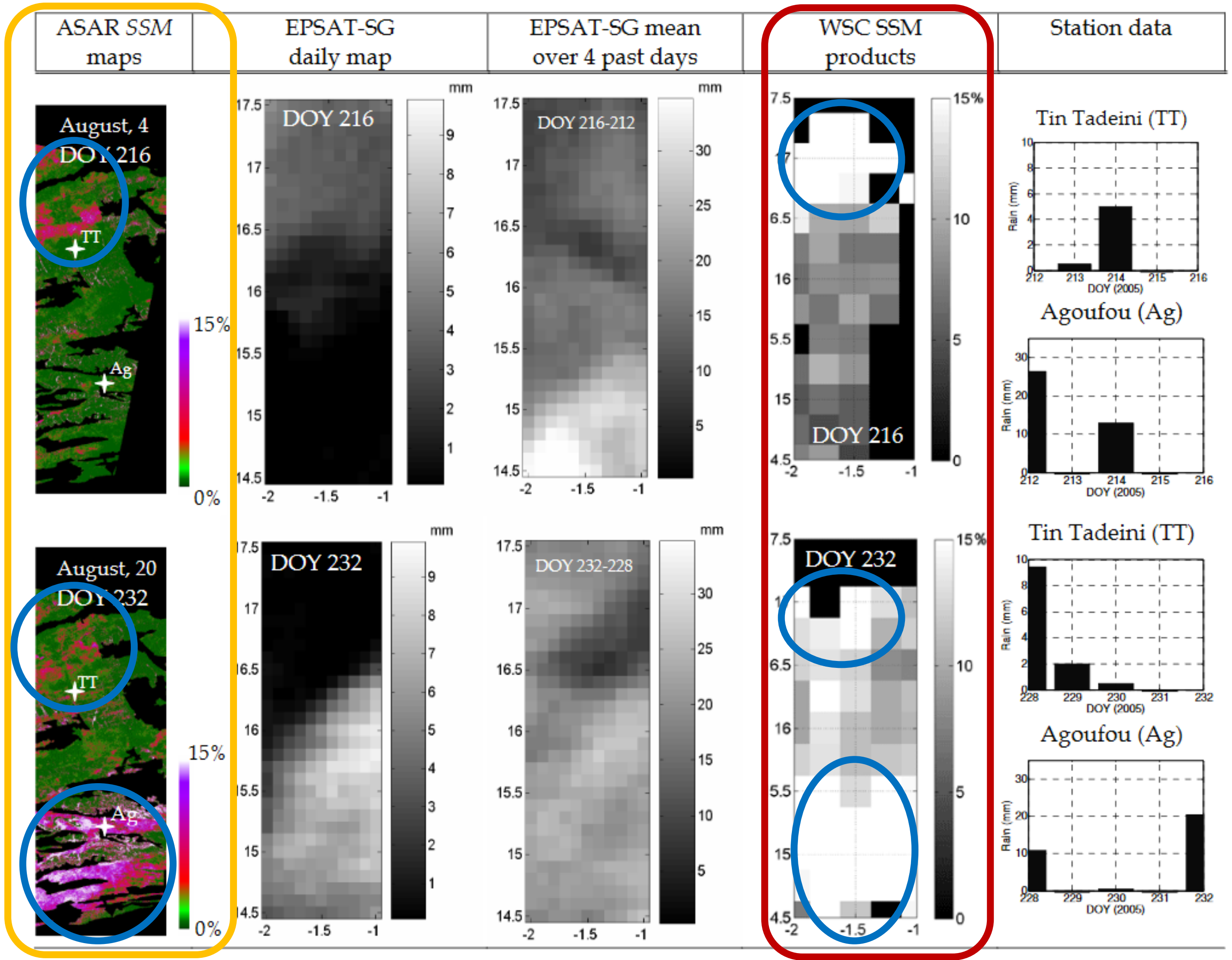

SSM derived from SAR (C-band) and scatterometer (C-band) over a semi-arid in Sahel (Gourma, Mali)

Wet areas

Baup et al., HESS (2011)

Major environmental applications of radar over land

- Vegetation water content (VWC) and biomass: Scatterometers and SAR

Vegetation optical depth: $VOD = -\frac{\cos\theta}{2}\ln\left(\frac{\sigma^{\circ}_{obs} - \sigma^{\circ}_{vege}}{C + D * SM - \sigma^{\circ}_{vege}}\right)$ Attema & Ulaby, Rad. Sci. (1978)

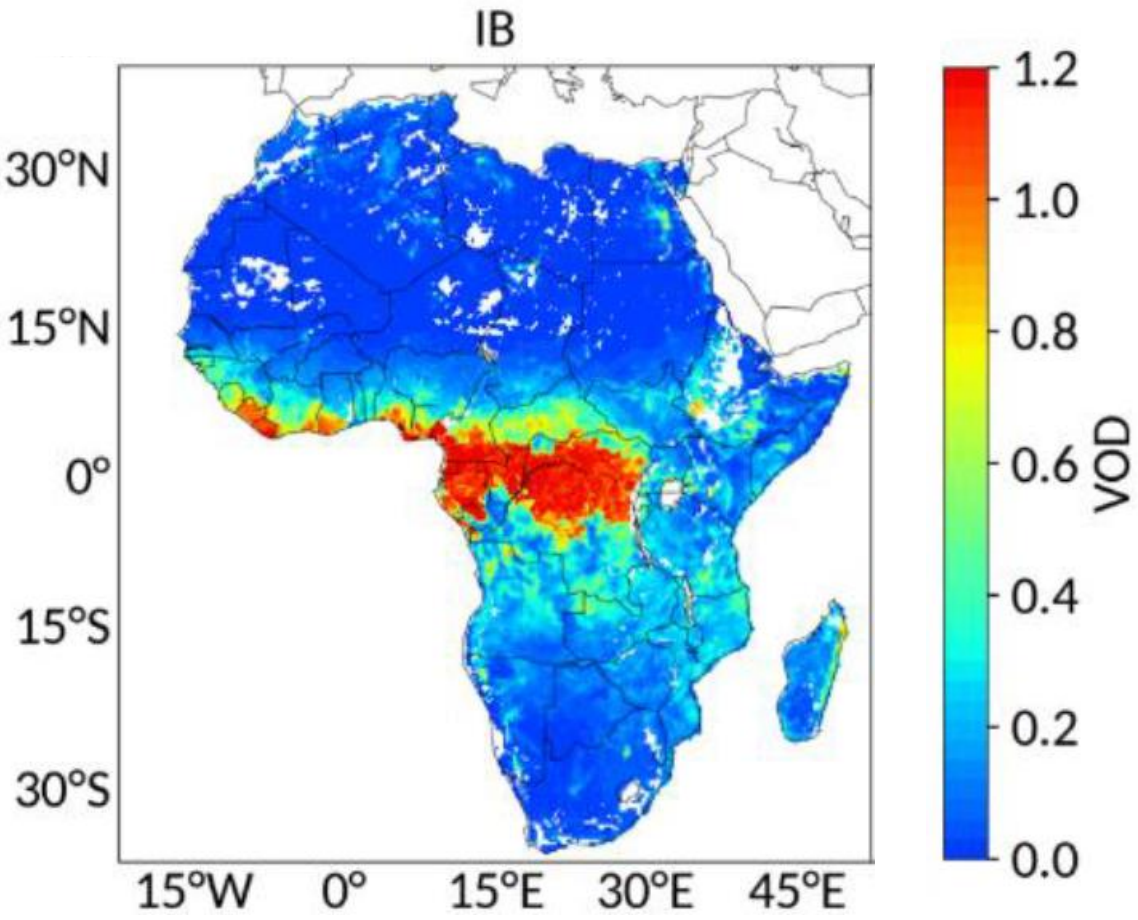

VOD averaged from 2015 to 2018 over Africa from ASCAT (C-band)

Liu et al., IEEE IGARSS (2020)

RSE (submitted)

IB: https://ib.remote-sensing.inrae.fr/

Major environmental applications of radar over land

- Flood mapping: SAR

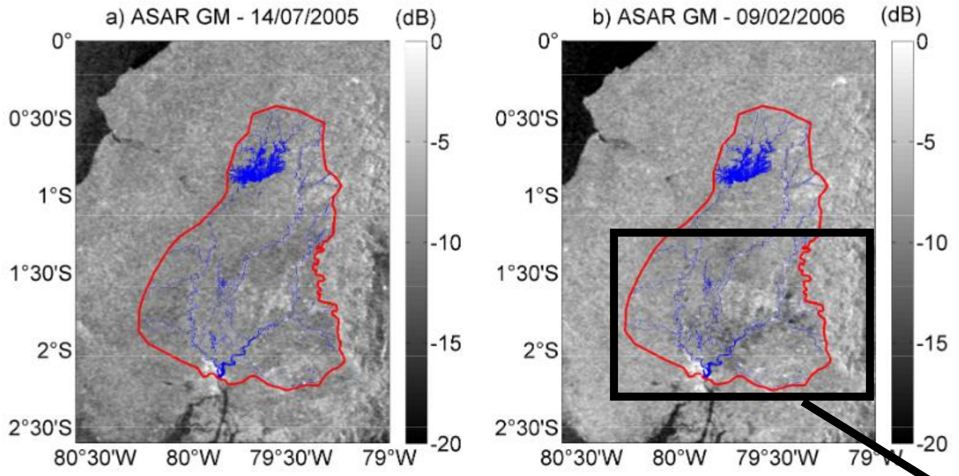

Detection change

ASAR (C-band) (2003-2008)

Annual frequency of inundation

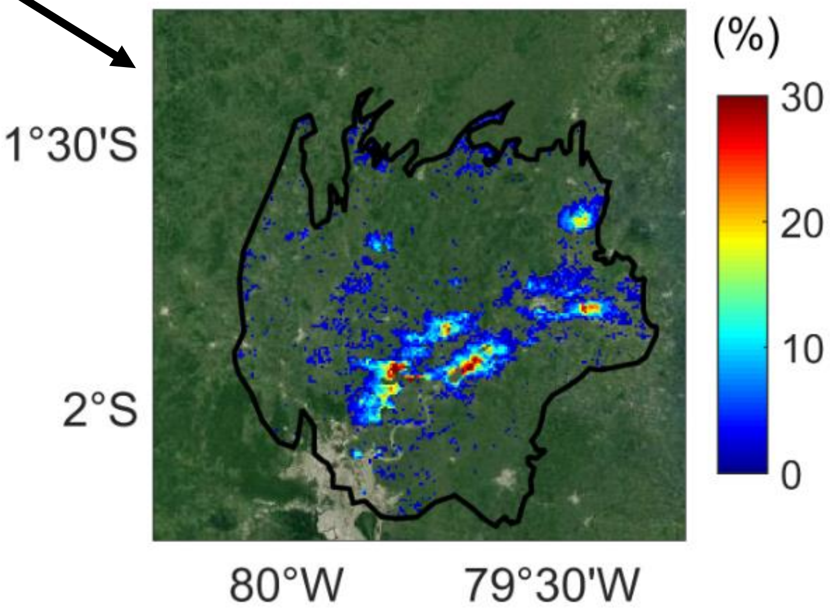

Monitoring of floods in large river basins: Guayas (Ecuador) 32,000 km²

Frappart et al., Water (2017)

Analysis of radar altimetry backscattering over land

- Global patterns of radar altimetry backscattering

S | Ku | Ka

Amplitude

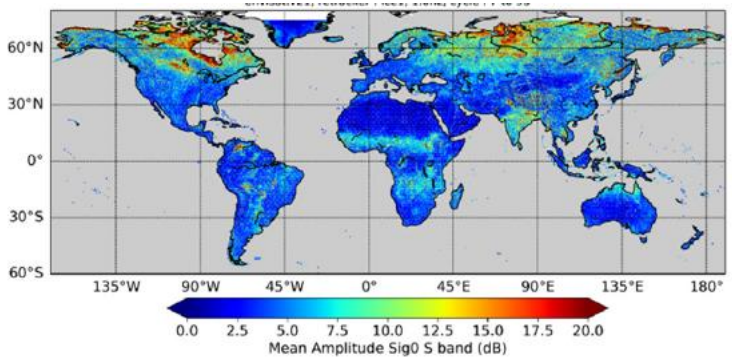

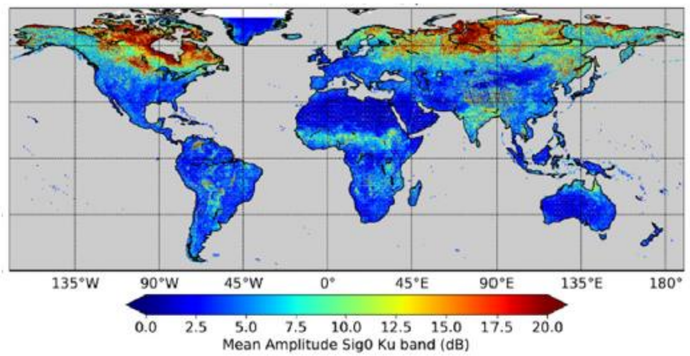

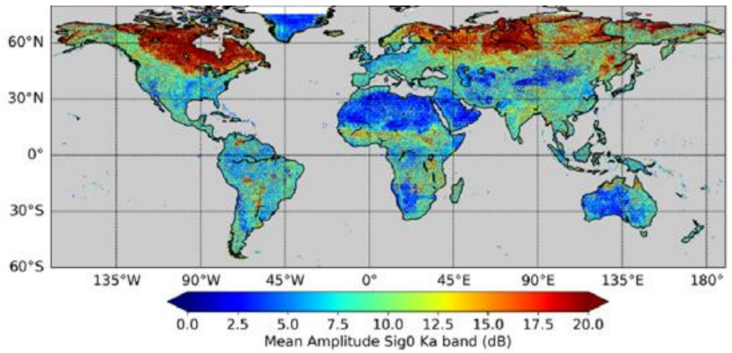

Month of occurrence of the maximum

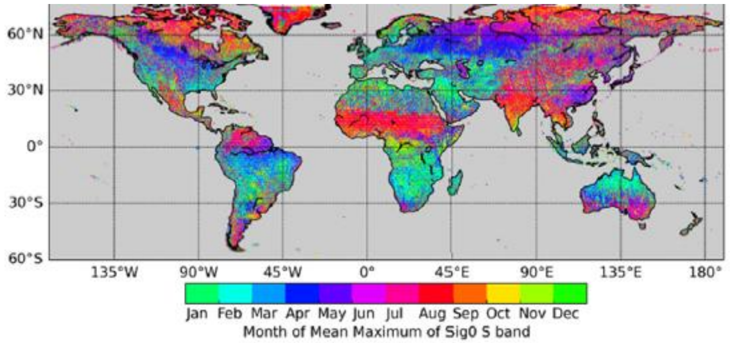

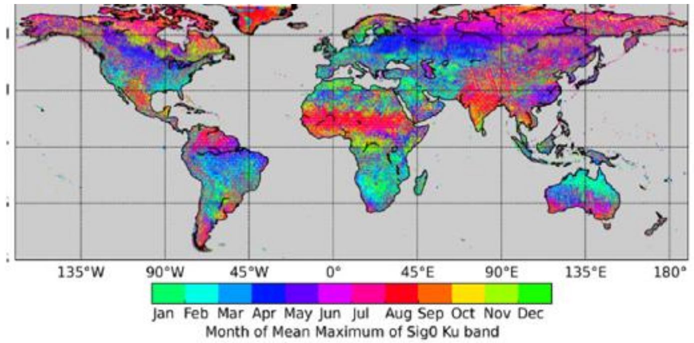

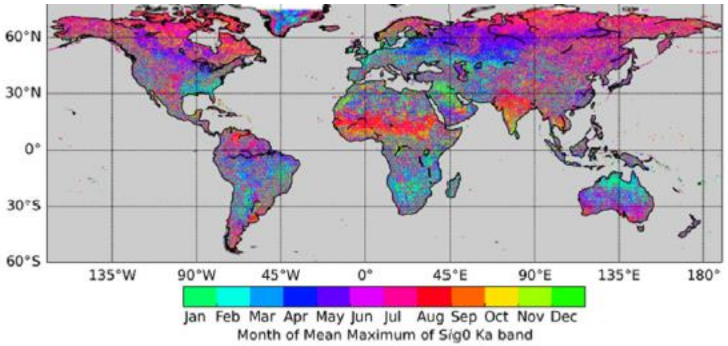

Frappart et al., ASR (in press)

Analysis of radar altimetry backscattering over land

- Comparison between backscattering at Ku-band from different radars

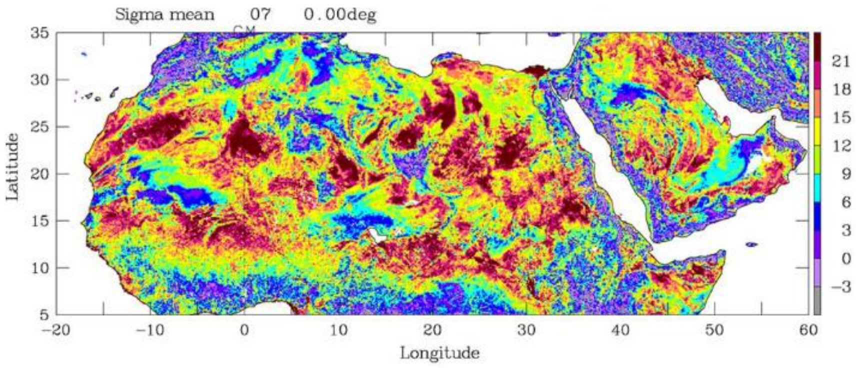

TRMM PR

(0°)

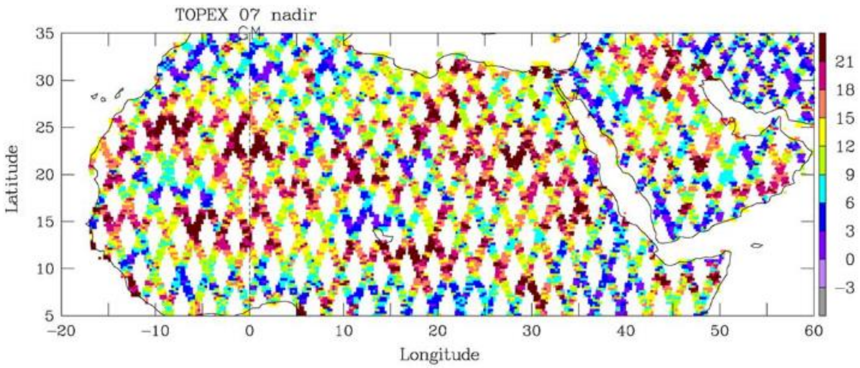

Topex

(0°)

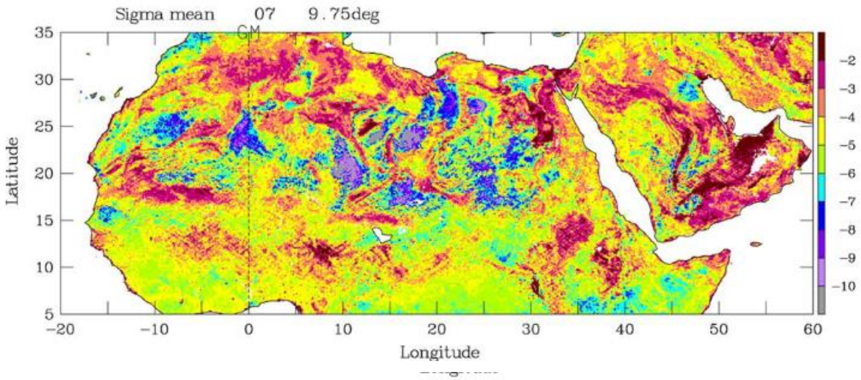

TRMM PR

(10°)

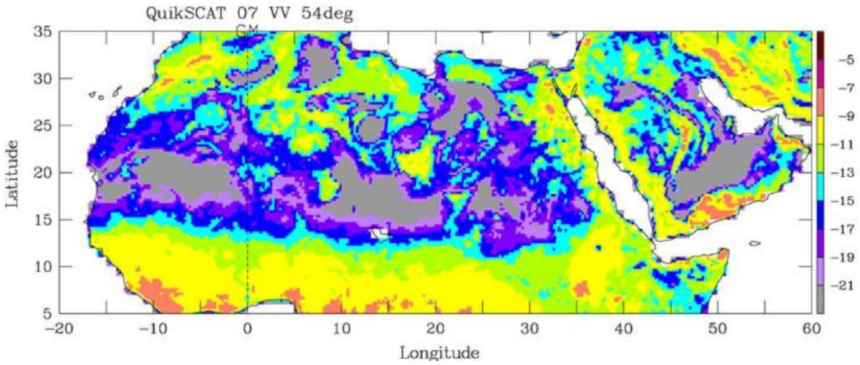

QuikSCAT

(54°, VV)

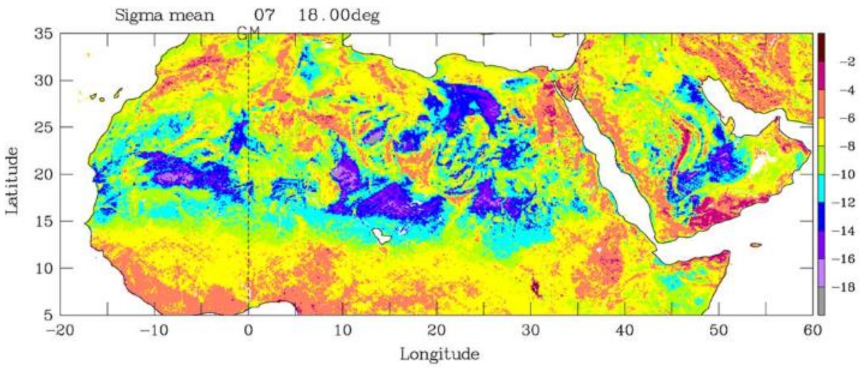

TRMM PR

(18°)

Prigent et al., IEEE TGARS (2015)

Analysis of radar altimetry backscattering over land

- Comparison between backscattering at Ku-band from different radars

Stone desert | Sahelian savannah | Equatorial forest

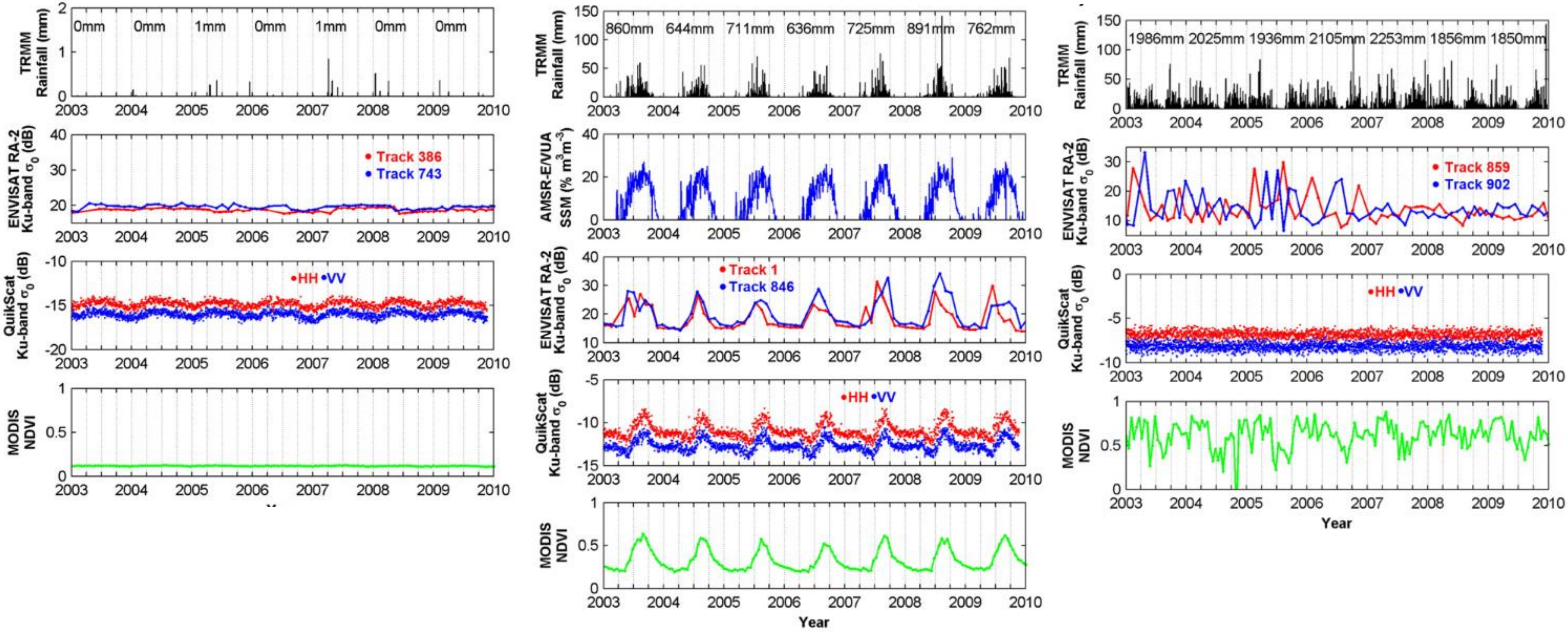

Fatras et al., RSE (2015)

Spatio-temporal variations of σ_0 from SWIM

Along SWIM ground-track 101

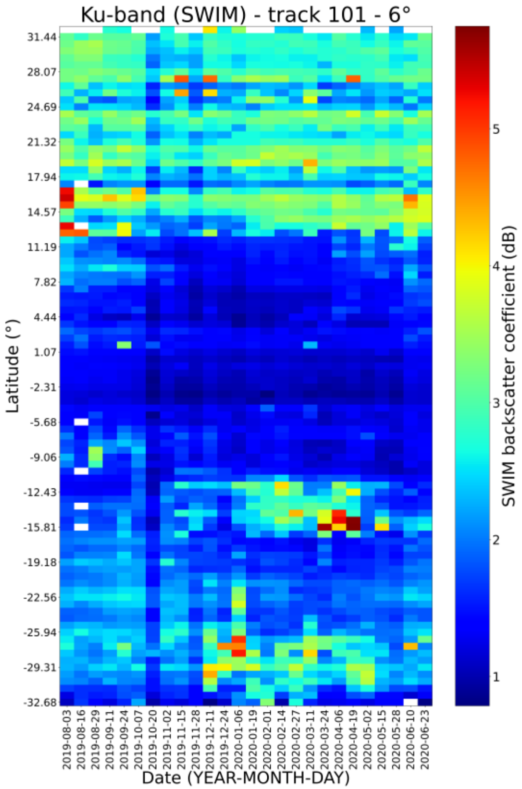

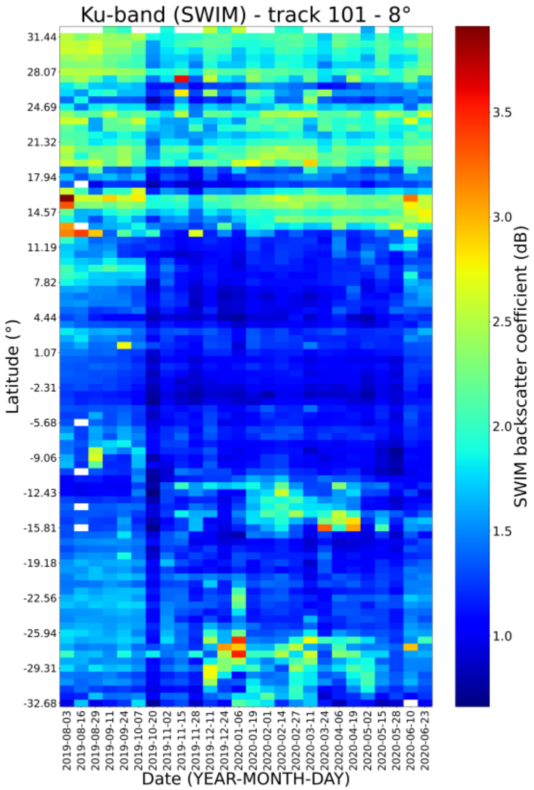

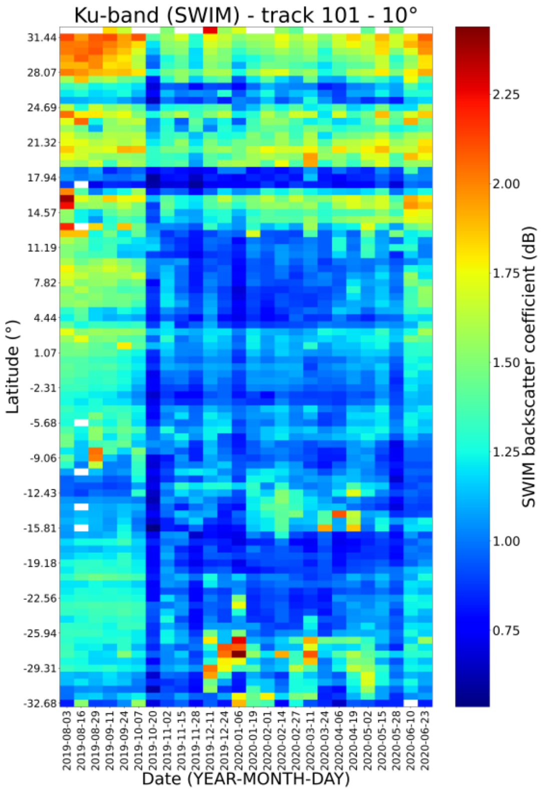

Spatio-temporal variations of σ_0 from SWIM

Along SWIM ground-track 101

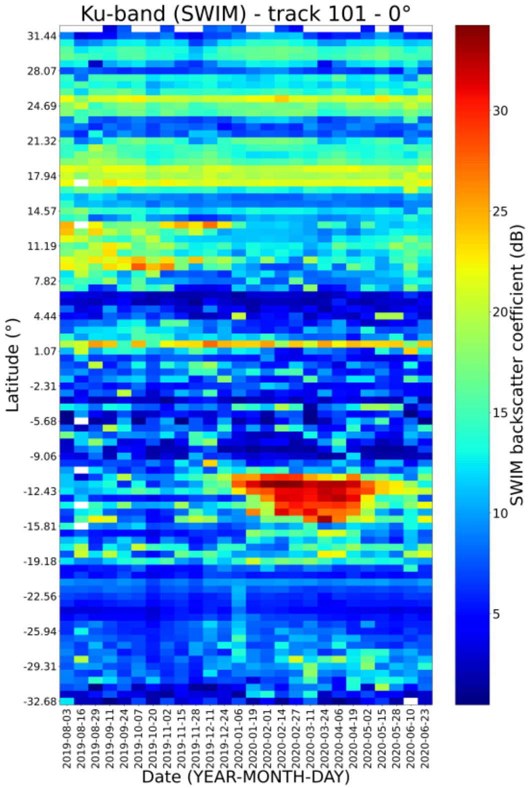

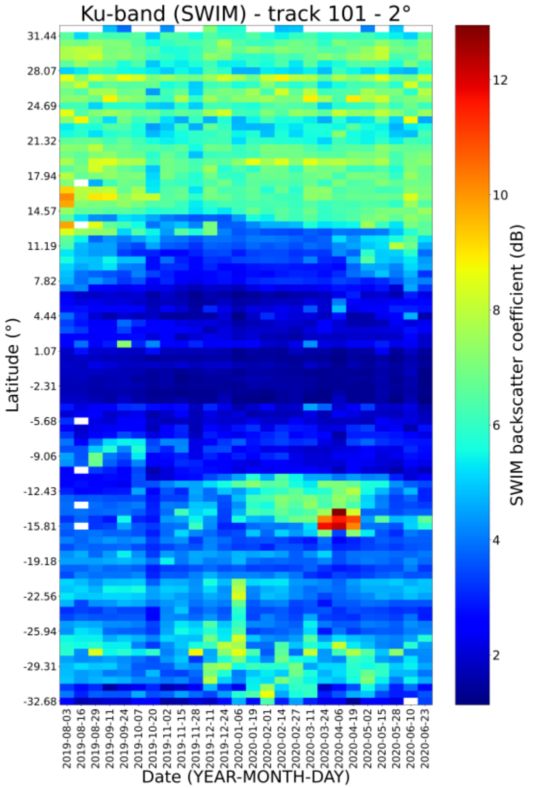

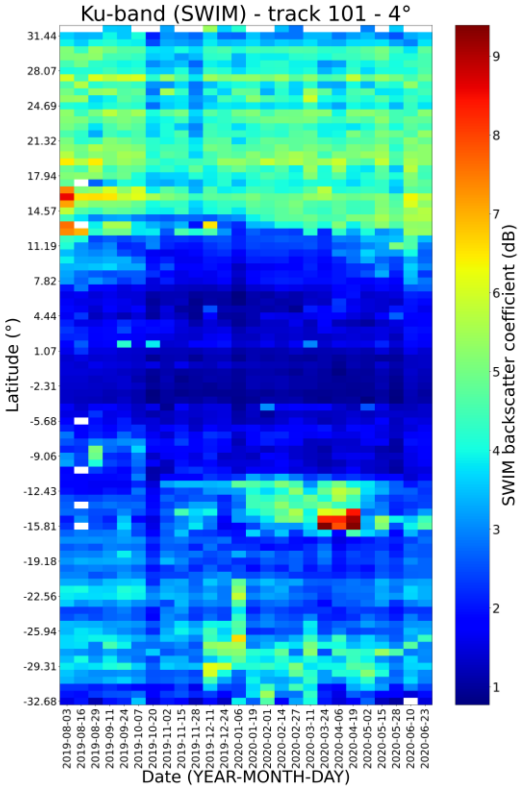

Results at continental scale

- Correlation between σ^0 from SWIM, SSM from ERA5, NDVI from MODIS

σ^0 (0°) from SWIM vs. SSM

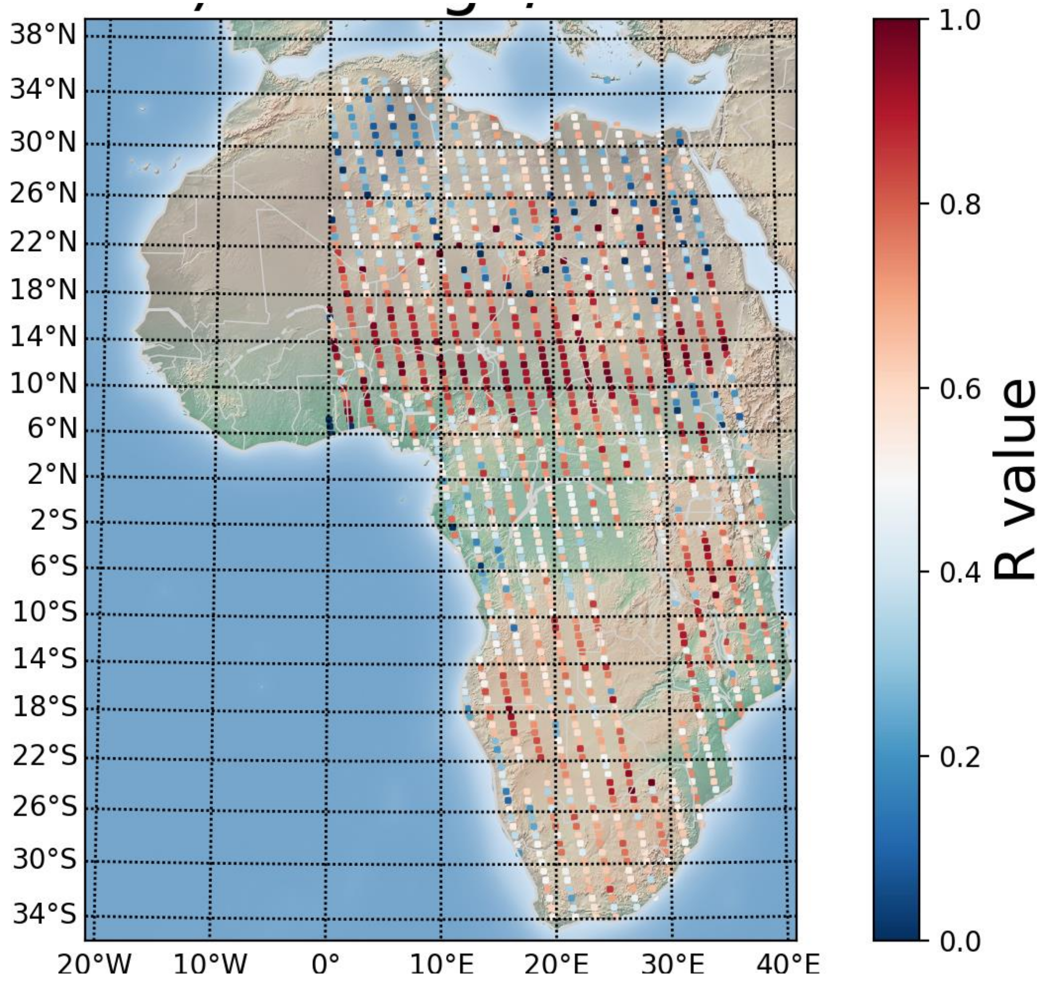

σ^0 (0°) from SWIM vs. NDVI

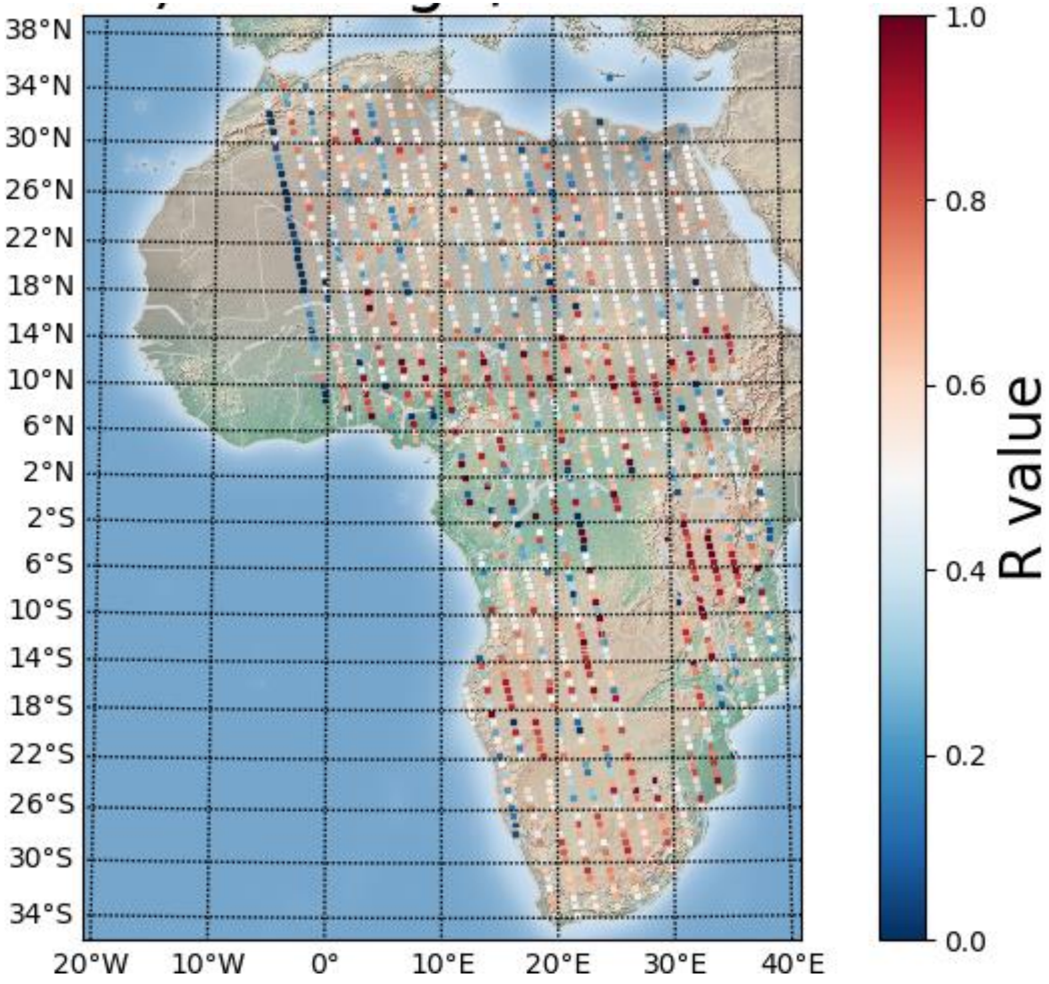

Frappart et al., Remote Sens. (2020)

Results at continental scale

- Correlation between σ^0 from SWIM, SSM from ERA5, NDVI from MODIS

σ^0 (10°) from SWIM vs. SSM

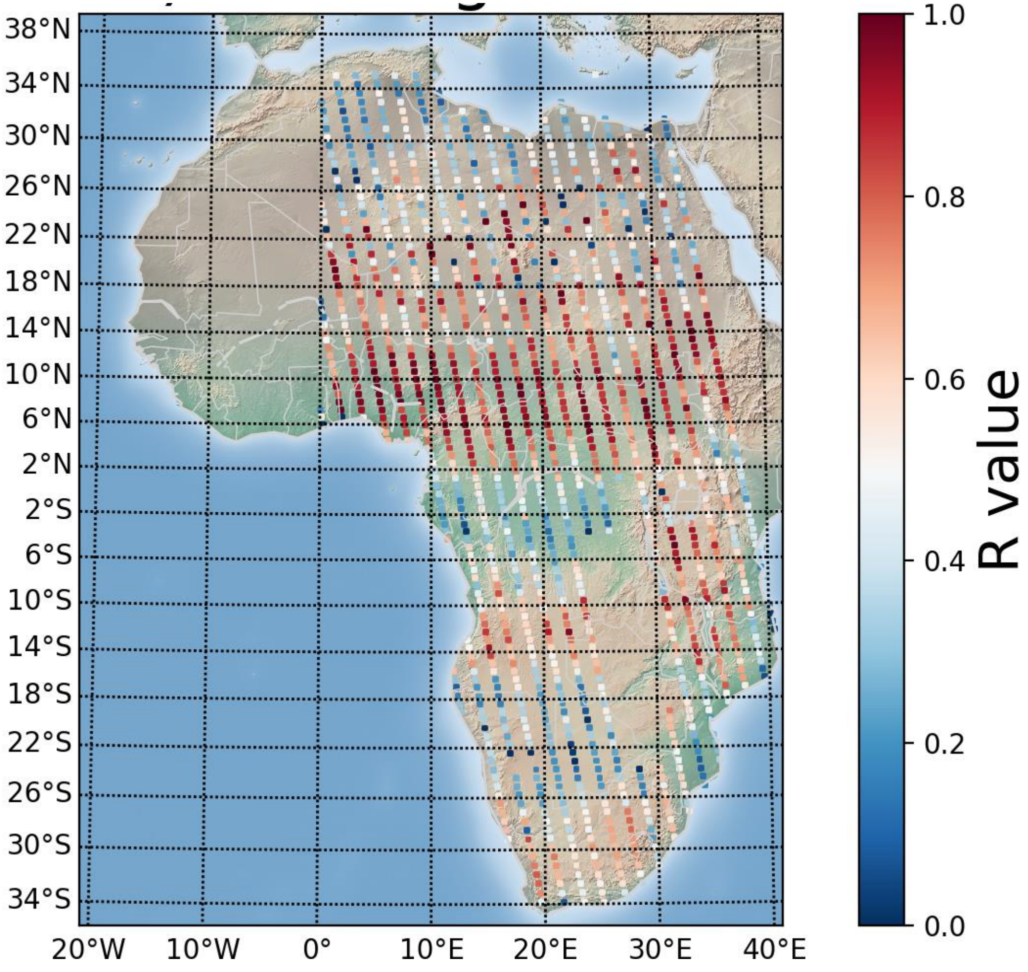

σ^0 (10°) from SWIM vs. NDVI

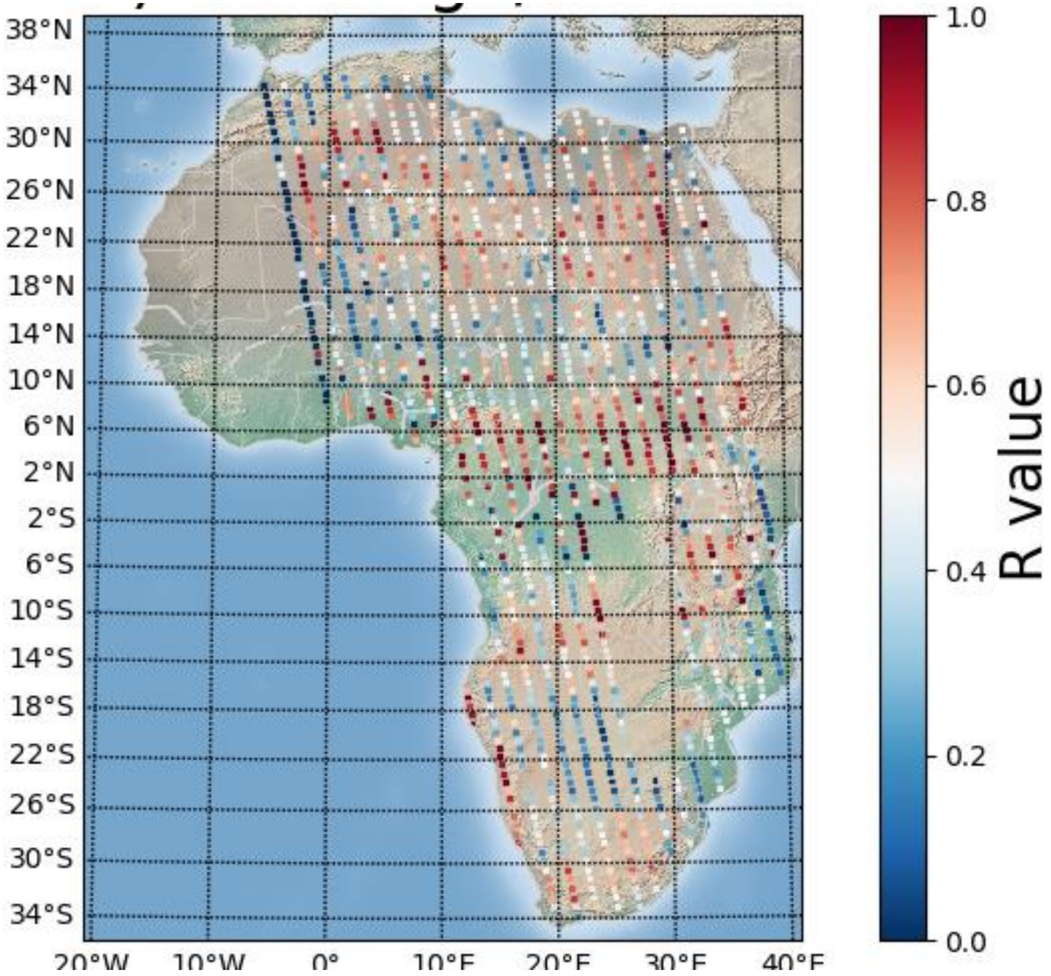

Frappart et al., Remote Sens. (2020)

Results at local scale

- sites with small changes in surface properties against time

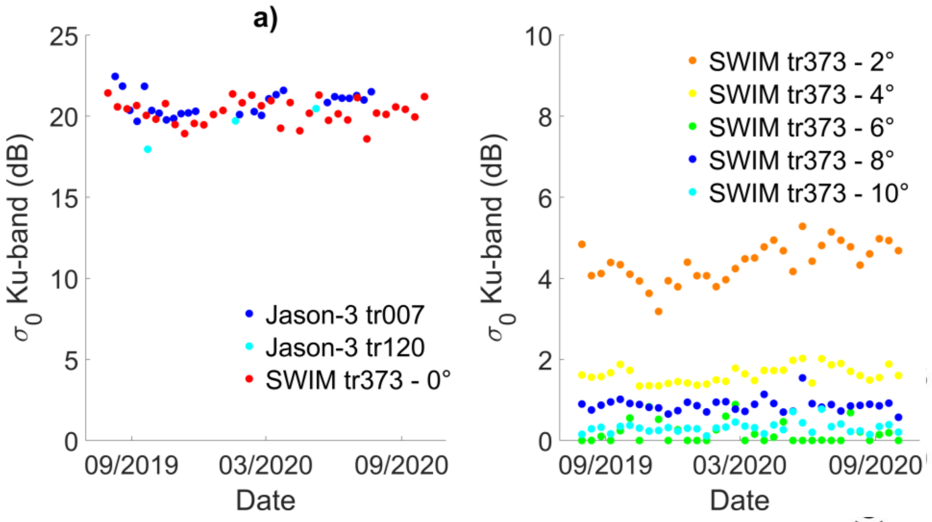

a) Stone desert

b) Sahelian savannah

c) Equatorial forest

Satellite	Stone desert		Sand desert		Rain forest	
	Mean (dB)	Std (dB)	Mean (dB)	Std (dB)	Mean (dB)	Std (dB)
Jason-3	20.1	1.0	17.4	0.6	3.0	0.9
SWIM 0°	20.3	0.7	14.5	1.2	4.9	1.5
SWIM 2°	4.4	0.5	5.9	0.5	1.4	0.1
SWIM 4°	1.6	0.2	2.6	0.4	1.4	0.1
SWIM 6°	0.2	0.3	0.4	0.5	0.1	0.1
SWIM 8°	0.9	0.2	0.8	0.2	0.1	0.1
SWIM 10°	0.3	0.1	0.5	0.1	0.1	0.1

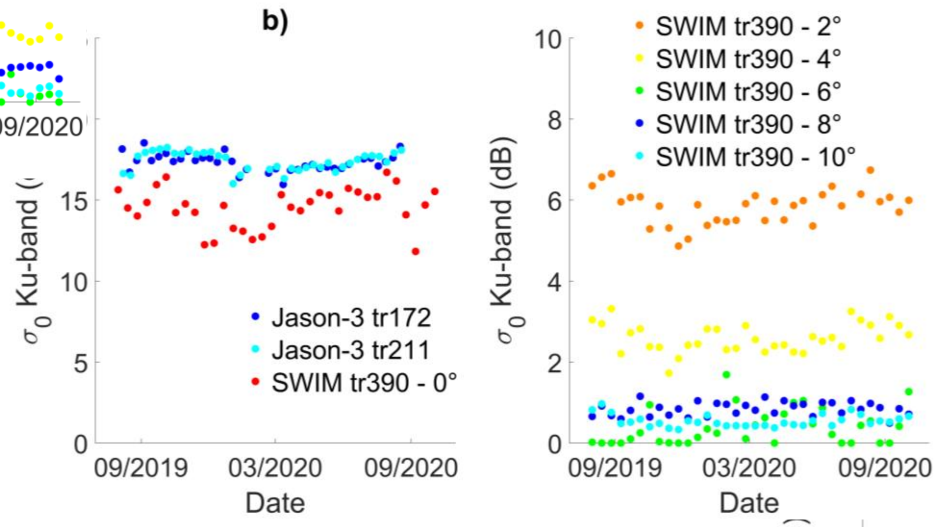

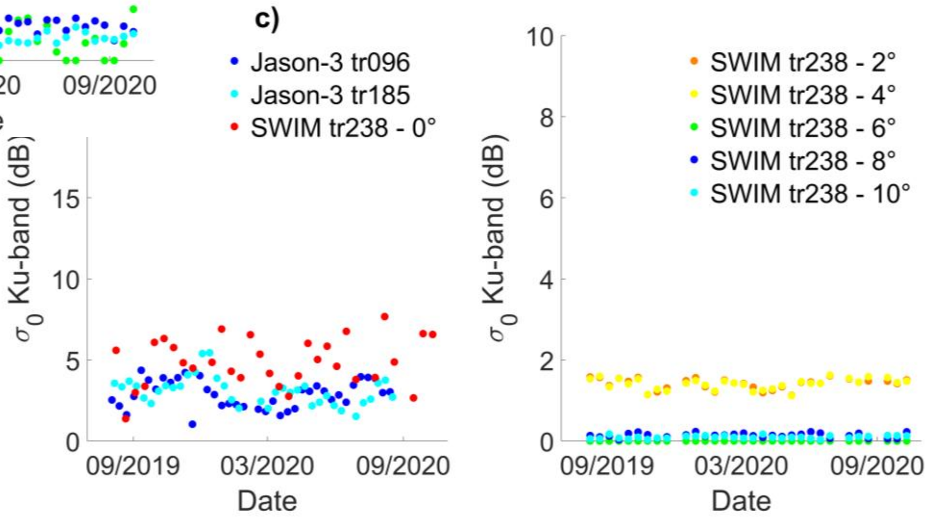

Frappart et al., IEEE IGARSS (submitted)

Results at local scale

- sites with temporal variations in surface properties

a) Soudano-Sahelian savannah

b) Inner Niger Delta floodplain

c) flooded Equatorial forest

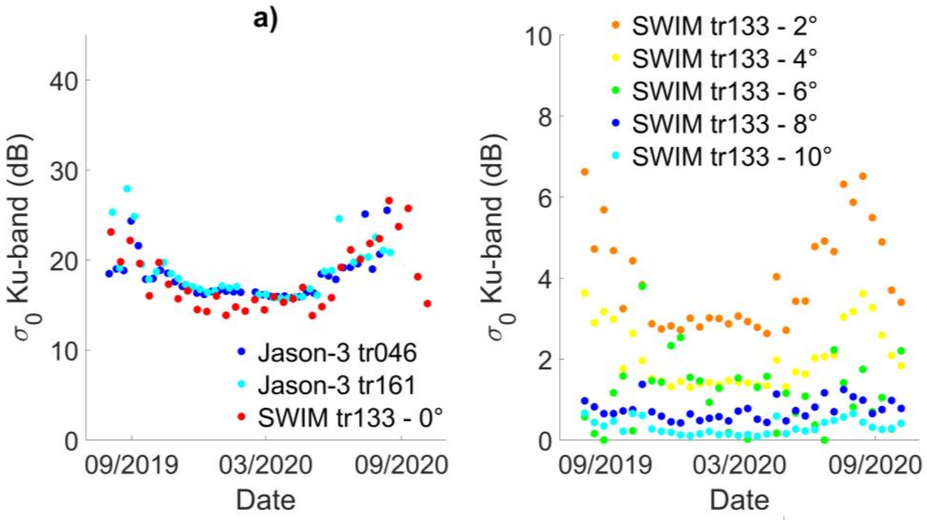

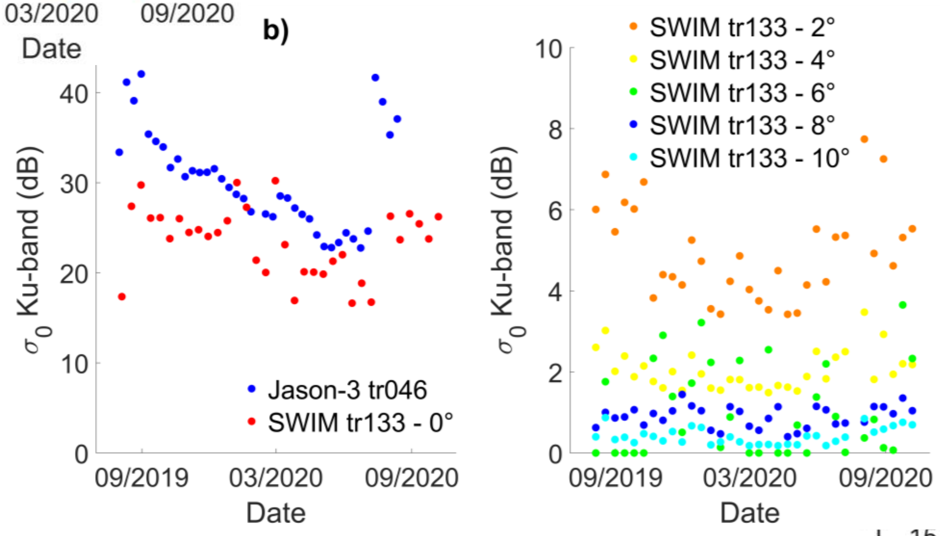

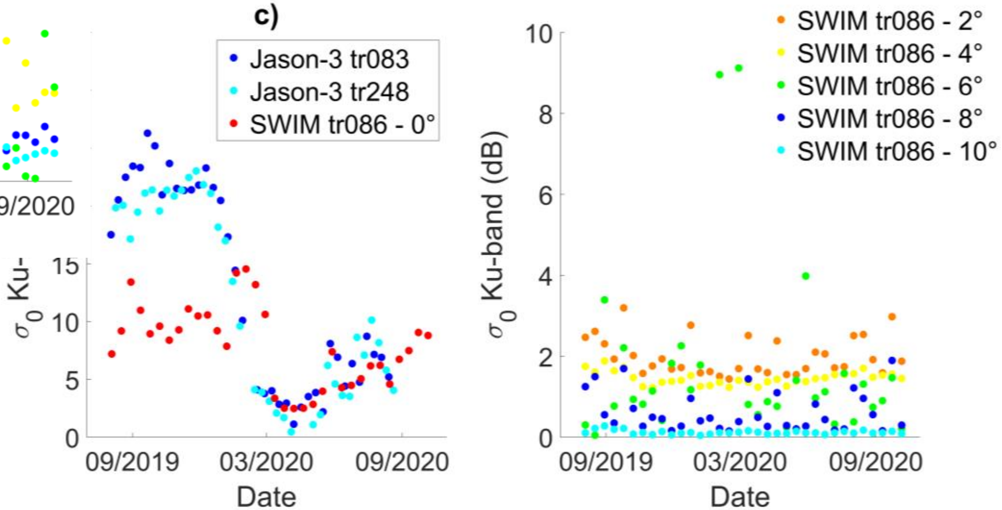

Frappart et al., IEEE IGARSS (submitted)

Conclusion & prospects

- Characterization of the spatio-temporal evolution of σ^0 as a function of the surface type and of the incidence

  (i.e., roughness, dielectral properties modified by change in wetness, …)

- Extend this study to SENTINEL-3 SAR altimeter and SCAT scatterometer data

- Invert SM and or VOD from SWIM and SCAT data

Thank you very much for your attention!

Radar Based Water Level Estimation

remote sensing

Guest Editors:

Dr. Frédéric Frappart

Dr. Isabel Vigo

Dr. Joana Fernandes

Dr. David García-García

Dr. José Darrozes

Dr. Fabien Blarel

Dr. Cassandra Normandin

Dr. Song Shu

Deadline for manuscript submissions:
30 September 2021

Message from the Guest Editors

Dear Colleagues,

This Special Issue aims to present reviews and recent advances of general interest in the use of radar for water level estimates. We encourage the submission of manuscripts presenting new methodology and new applications of radar techniques including GNSS, GNSS-R, radar altimetry, and especially from recent altimetric technology (SAR, SARin and Ka band) and improvements expected from missions to be launched in the near future (i.e., SWOT), or analyzing the accuracy of radar techniques for water level estimates.

- water levels
- ocean dynamic topography
- surface water topography
- radar
- altimetry
- InSAR
- GNSS
- GNSS-R
- floodplain water volume
- river bank topography changes

https://www.mdpi.com/journal/remotesensing/special_issues/Radar_Based_Water_Level_Estimation

frederic.frappart@legos.obs-mip.fr